

# Correlated Trapped Bosons and the Many-Body Efimov Effect

O. Sørensen, D. V. Fedorov, and A. S. Jensen

*Institute of Physics and Astronomy, University of Aarhus, DK-8000 Aarhus C, Denmark*

(Dated: November 4, 2018)

We study two-body correlations in systems of identical bosons. We use a Faddeev type of decomposition of the wave function where all pairs of particles are treated equally. We focus on a new multi-particle Efimov effect at large scattering length, where infinitely many loosely bound many-body states appear. A confining external trap only allows a finite number of such spatially extended negative energy states inside the trap. The stability of a Bose condensate is determined by the decay into these model independent intermediate states which in turn decay into dimers.

PACS numbers: 31.15.Ja, 05.30.Jp, 21.65.+f

*Introduction.* The novel theoretical formulation in [1] was constructed to describe correlations in boson systems and applied for a realistic short-range repulsive interaction to Bose-Einstein condensates. The method goes beyond the mean-field approximation [2, 3] and is as well applicable to attractive finite range potentials with very large scattering lengths where the Efimov effect occurs [4, 5]. Experimental properties are available for various condensates from the first observations of both effectively repulsive [6] and attractive [7] interatomic interactions to the recent observations [8, 9] of condensates in a magnetic field used to tune the effective interaction via a Feshbach resonance to almost any scattering length.

The condensate [2] being an excited state of the full many-body system is clearly unstable. The three-body recombination into bound dimers is a dominating decay channel [10, 11, 12]. In the condensate this occurs independently for neighbouring pairs and much more frequently in a coherent process best described as a collective or macroscopic collapse [13, 14]. Two-body correlations therefore must be crucial for this collapse, which becomes more likely and eventually inevitable as the scattering length is increased. Unfortunately a theoretical description is hindered by the difficulties, especially pronounced for large scattering lengths, of finding the decisive correlated structure [2, 15, 16].

A promising form of a correlated wave function suggested for nucleons [17] was recently extended to more general systems [18]. Another related formulation uses generalized hyperspherical coordinates and an adiabatic expansion with the hyperradius as the adiabatic coordinate [19]. It was applied for many identical bosons, still only with a zero-range interaction and the lowest (constant and thus non-correlated) hyperspherical angular wave function. These crude approximations are removed in a novel method still using hyperspherical coordinates and adiabatic expansion, but now the wave function is determined from a variationally established equation [1]. The purpose of this letter is to investigate the structure of boson systems as a function of (large) scattering length for attractive finite range potentials with emphasis on an emerging novel many-body Efimov effect.

*Theory.* A system of  $N$  identical particles of masses  $m$ , trapped in an external field approximated by a harmonic oscillator potential of angular frequency  $\omega$ , can in the center of mass frame be described by hyperspherical coordinates, i.e.  $3N - 4$  hyperangles [18, 20] denoted collectively by  $\Omega$  and one hyperradius,  $\rho$ , given by [1]

$$\rho^2 = \frac{1}{N} \sum_{i < j=1}^N r_{ij}^2 = \sum_{i=1}^N r_i^2 - NR^2, \quad (1)$$

where  $\vec{r}_i$  are single-particle coordinates,  $\vec{R}$  is the center of mass coordinate, and  $r_{ij} = |\vec{r}_j - \vec{r}_i| \equiv \sqrt{2\rho} \sin \alpha_{ij}$  with  $\alpha_{ij}$  varying between 0 and  $\pi/2$ . The hamiltonian is

$$\hat{H} = \sum_{i=1}^N \left( \frac{\hat{p}_i^2}{2m} + \frac{1}{2}m\omega^2 r_i^2 \right) + \sum_{i < j=1}^N V(r_{ij}), \quad (2)$$

where  $V$  is the two-body interaction. It separates into a center of mass part, a radial part, and an angular part depending respectively on  $\vec{R}$ ,  $\rho$ , and  $\Omega$  [1]:

$$\hat{H} = \hat{H}_{\text{cm}} + \hat{H}_\rho + \frac{\hbar^2 \hat{h}_\Omega}{2m\rho^2}, \quad (3)$$

with  $\hat{H}_{\text{cm}} = \hat{p}_R^2/(2Nm) + Nm\omega^2 R^2/2$ ,  $\hat{H}_\rho = \hat{T}_\rho + m\omega^2 \rho^2/2$  and  $\hbar^2 \hat{h}_\Omega/(2m\rho^2) = \hat{T}_\Omega + \sum_{i < j} V_{ij}$ , where  $\hat{T}_\rho$  and  $\hat{T}_\Omega$  are related kinetic energy operators. A suitable expansion of the wave function is

$$\Psi = \rho^{-(3N-4)/2} \sum_{n=0}^{\infty} f_n(\rho) \Phi_n(\rho, \Omega), \quad (4)$$

where  $\Phi_n$  is an eigenfunction of the angular part of the hamiltonian with an eigenvalue  $\hbar^2 \lambda_n(\rho)/(2m\rho^2)$ :

$$\hat{h}_\Omega \Phi_n(\rho, \Omega) = \lambda_n(\rho) \Phi_n(\rho, \Omega). \quad (5)$$

Neglecting couplings between the different  $n$ -channels yields the radial eigenvalue equation for the energy  $E_n$ :

$$\left( -\frac{\hbar^2}{2m} \frac{d^2}{d\rho^2} + U_n(\rho) - E_n \right) f_n(\rho) = 0, \quad (6)$$

$$U_n(\rho) = \frac{m\omega^2 \rho^2}{2} + \frac{\hbar^2(3N-4)(3N-6)}{8m\rho^2} + \frac{\hbar^2 \lambda_n}{2m\rho^2}. \quad (7)$$

The second term in the radial potential  $U$  is a generalized centrifugal barrier. We now decompose the angular wave function  $\Phi$  in the symmetric Faddeev components  $\phi$

$$\Phi(\rho, \Omega) = \sum_{i < j=1}^N \phi_{ij}(\rho, \Omega) \approx \sum_{i < j=1}^N \phi(\rho, r_{ij}), \quad (8)$$

where the restricting assumption is that the interparticle potentials only act in  $s$ -waves leaving only the dependence on the distance  $r_{ij} = \sqrt{2}\rho \sin \alpha_{ij}$ . The capability of this decomposition for large scattering length has been demonstrated for  $N = 3$  by the proper description of the intricate Efimov effect [5, 21].

The eigenvalue equation eq. (5) can by a variational technique be rewritten as a second order integro-differential equation in the variable  $\alpha_{12}$  [1]. For atomic condensates the interaction range is very short compared to the spatial extension of the  $N$ -body system. Then this equation simplifies even further to contain at most one-dimensional integrals. The principal interaction dependence is through the parameter  $a_B \equiv m \int_0^\infty dr r^2 V(r)/\hbar^2$ , which is the Born-approximation to the  $s$ -wave scattering length  $a_s$ . The validity of our approximations only relies on a small range of the potential whereas the scattering length can be as large as desired.

*Angular potentials.* The crucial ingredient is the angular eigenvalue  $\lambda$  obtained from eq. (5). We choose gaussian two-body potentials  $V(r) = V_0 \exp(-r^2/b^2)$  of range  $b$  and strength  $V_0$ . We measure lengths in units of  $b$  and energies in units of  $\hbar^2/(2mb^2)$ . We solve the equation by choosing discrete sets of mesh points and thus constructing a matrix equation ready for diagonalization [1]. This computational scheme increases strongly with  $N$  and we therefore illustrate by relatively small values of  $N$ .

Fig. 1 shows the angular eigenvalues for different strengths expressed in terms of  $a_B$  and  $a_s$ . For short range potentials finite at the origin all  $\lambda$  approach their values at  $\rho = 0$  as  $\rho^2$ . This is a model dependent region and therefore not considered in the following. When the potential is too weak to support a two-body bound state, ( $a_B/b > -1.18934$ ), the lowest  $\lambda_0$  is negative and approaches zero as  $a_s/\rho$  with increasing  $\rho$ . In fig. 1 we also show the eigenvalue  $\lambda_1$  corresponding to the first excited angular state. It is positive and approaches the value  $4(4 + 3N - 5)$  as  $-a_s/\rho$  for large  $\rho$  [19, 21].

Increasing the attraction of the potential a two-body bound state of energy  $B_2$  appears (positive  $a_s$ ) and the corresponding lowest angular eigenvalue diverges proportional to  $2mB_2\rho^2/\hbar^2$  when  $\rho \rightarrow \infty$ . The many-body system would obviously then prefer to recombine into bound dimer states. The first excited angular eigenvalue, similar to the dotted curve in fig. 1, is then responsible for the unstable state referred to as the condensate.

At the two-body threshold the scattering length is infinite. Then the lowest  $\lambda$  approaches a negative constant  $\lambda_\infty$  for large  $\rho$  ( $\rho \gtrsim \rho_b \equiv 45\sqrt{N}b$ ), see fig. 1. Using

$N = 3, 10, 20$  we find numerically  $\lambda_\infty(N) \approx 24(N - 2) - 5N(N - 1)$ , where the form reflects our expectations of  $N$ -dependence of kinetic and potential energies.

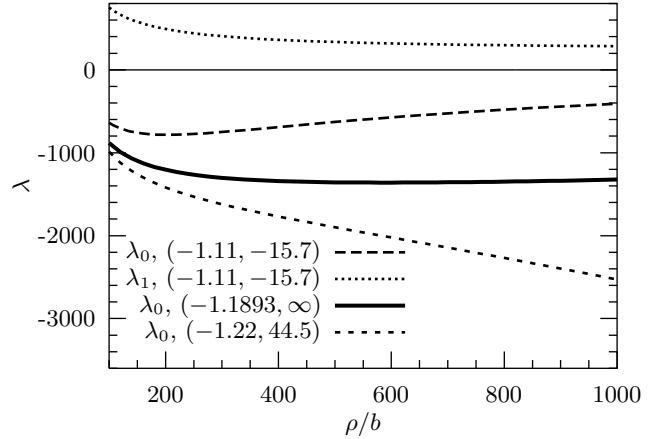


FIG. 1: Angular eigenvalues as functions of  $\rho$  for  $N = 20$  and various potential strengths given by  $(a_B/b, a_s/b)$ . The long-dashed and the dotted curves correspond to the two lowest eigenvalues when the two-body potential is too weak to support a bound state. The potential giving rise to the short-dashed curve has only one bound two-body state and the solid curve corresponds to the two-body threshold of zero energy.

These angular eigenvalues behave qualitatively different from those obtained in [19], where the expectation value of a  $\delta$ -interaction of strength proportional to  $a_s$  is computed with a constant angular wave function without any correlations. The eigenvalues are then necessarily proportional to  $a_s/\rho$  for all  $\rho$ , i.e. always diverging when  $\rho \rightarrow 0$  and converging to zero for  $\rho \rightarrow \infty$ . The differences are especially pronounced for large scattering lengths and when a bound two-body state is present. However, even in the qualitatively similar case in fig. 1 of  $a_s/b = -15.7$  our  $\lambda$  is lower than that of [19] by a factor between 1.5 and 2 for  $\rho/b \in [10^3, 10^5]$ .

At large  $\rho$ ,  $\Phi$  approaches a non-correlated angular wave function. Using a constant as in [19] the expectation value of our gaussian interaction gives for large  $\rho$  and  $N$  that  $\lambda = \lambda_{n-c}(\rho) \equiv kN^{7/2}a_B/\rho$  with  $k = (3/2)^{3/2}/\sqrt{2\pi}$ , i.e. we get  $a_B$  instead of  $a_s$  as assumed in [19]. For large  $a_s$  our computed  $\lambda$  bends upwards from the plateau of  $\lambda_\infty$  around a point  $\rho \equiv \rho_{th}$  determined by the large but finite value of  $a_s$ . If  $\rho > \rho_{th}$  then  $\lambda$  can be estimated as  $\lambda_{n-c}(\rho)$  with  $a_s$  substituted for  $a_B$ . The transition point is then given by  $\lambda_\infty = \lambda_{n-c}(\rho_{th})$  which for large  $N$  yields

$$\rho_{th} = \frac{1}{5}k|a_B|N^{3/2} \simeq \frac{1}{7}|a_B|N^{3/2} \rightarrow \frac{1}{7}|a_s|N^{3/2}, \quad (9)$$

where the more realistic estimate for attractive potentials is indicated by exchanging  $a_B \rightarrow a_s$ , see [19, 21].

*Radial potentials.* In eq. (7) the external harmonic trap of angular frequency  $\omega$  corresponds to a trap length  $b_t \equiv \sqrt{\hbar/(m\omega)}$ . We model the experimentally studied

systems [6, 9] of  $^{85}\text{Rb}$  and  $^{87}\text{Rb}$ -atoms with oscillator frequencies  $\nu = \omega/(2\pi) = 205$  Hz and 200 Hz and interaction range  $b = 10$  a.u., thus yielding  $b_t/b = 1442$ .

We show in fig. 2 the radial potentials for the angular eigenvalues corresponding to unbound two-body systems ( $a_s/b = -15.7$  in fig. 1). The external field in eq. (7) is negligible for small  $\rho$  and therefore the radial potential is negative when  $\lambda + (3N - 4)(3N - 6)/4 < 0$ . Then genuinely bound states of negative energy are possible in our model without the confinement from the trap.

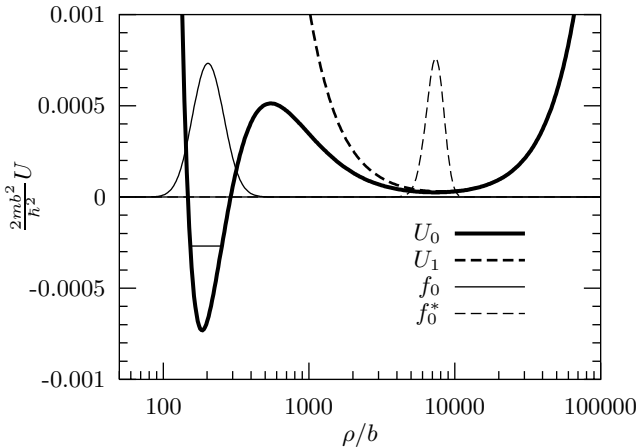


FIG. 2: Radial potentials  $U_0$  and  $U_1$  from eq. (7) corresponding to the two lowest angular potentials for  $N = 20$  and  $a_s/b = -15.7$  in fig. 1. The trap length is  $b_t/b = 1442$ . Also shown are the two lowest energies and the radial eigenfunctions  $f_0$  and  $f_0^*$  for the lowest radial potential.

The radial potential for the lowest angular eigenvalue has a global minimum with  $U_{\min} < 0$  at small  $\rho$  ( $\approx \rho_b$ ) separated by a barrier at intermediate  $\rho$  from a local minimum at  $\rho \sim \rho_t \equiv \sqrt{3N/2} b_t$ . At large  $\rho$  the radial potential diverges due to the harmonic term, at small  $\rho$  due to the centrifugal term. The radial potential corresponding to the first excited angular state, also in fig. 2, coincides with the lowest radial potential at large  $\rho$ , but does not contain the attraction at small  $\rho$  (see fig. 1) and diverges therefore to  $+\infty$  for small  $\rho$  without going through another minimum.

The radial equation in eq. (6) has only one solution with negative energy  $E$  and the corresponding wave function, shown in fig. 2, is located in the global minimum. The first of the infinitely many excited states in this potential is located in the local minimum at larger  $\rho$  created by the competition between the centrifugal barrier and the external harmonic oscillator potential. This excited state is usually referred to as the condensate, but the moderate attraction for the relatively small  $a_s = -15.7$  already results in a lower lying many-body state about  $\rho_t/\rho_b \approx 37$  times smaller than the condensate.

*Large scattering length.* At the threshold for binding of the two-body system the angular eigenvalue outside the interaction range must approach a negative constant

$\lambda \rightarrow \lambda_\infty$ , see fig. 1. The scattering length is then infinitely large and the radial potential has the form [22]

$$U(\rho) \rightarrow \frac{\hbar^2}{2m} \left( \frac{-\xi^2 - 1/4}{\rho^2} + \frac{\rho^2}{b_t^4} \right), \quad (10)$$

where  $\xi^2 \equiv -\lambda_\infty - (3N - 4)(3N - 6)/4 - 1/4 \approx 11N^2/4$  for large  $N$ , where  $\lambda_\infty \approx -5N^2$ . Without the external  $\rho^2$  potential in eq. (10) the infinitely many radial solutions to eq. (7) all behave like

$$f_\infty(\rho) = \sqrt{\rho} \sin(|\xi| \ln(\rho/\rho_{\text{sc}})), \quad (11)$$

with some hyperradius scale  $\rho_{\text{sc}}$ . The energies and sizes of the eigenstates labeled  $j$  are related by [4, 22]

$$\frac{E_j}{E_{j+1}} = \frac{\langle \rho^2 \rangle_{j+1}}{\langle \rho^2 \rangle_j} = e^{2\pi/|\xi|}. \quad (12)$$

With increasing quantum number these states become exponentially larger with exponentially smaller energies approaching zero. They originate from the constant  $\lambda$  and the generic  $1/\rho^2$  potential in eq. (10). They are many-body states, but not the embedded three-body Efimov cluster states which also arise from a  $1/\rho^2$  potential. However, both multi- and three-body Efimov states appear for very large two-body scattering lengths.

The external harmonic oscillator limits the possible number of these new states with  $E < 0$ . These negative energy states have to be located inside the trap and outside the two-body potential. The number of nodes of  $f_\infty$  allowed in this region equals the number of bound states  $N_E \approx |\xi| \pi^{-1} \ln(\rho_{\text{max}}/\rho_{\text{min}})$ , where the first and last zero points then are at the end points of the interval. We obtain  $\rho_{\text{max}}/\rho_{\text{min}} \approx \rho_t/\rho_b$  (see also fig. 3)

$$N_E \approx \frac{|\xi|}{\pi} \ln \left( \frac{b_t}{37b} \right), \quad \text{for } b_t \ll N|a_s|, \quad (13)$$

where the quoted condition of validity is found from  $\rho_t \ll \rho_{\text{th}}$ , i.e. the plateau value must extend beyond the trap. The number of these available Efimov states therefore scales proportional to  $N$  ( $\xi \propto N$ ) and logarithmically with the ratio of trap length and interaction range.

We show in fig. 3 the radial potential for  $N = 20$  and infinite scattering length corresponding to  $\lambda_\infty \sim -1340$  or  $\xi^2 \sim 584$ , see fig. 1. Using the estimate in eq. (13) we get  $N_E \approx 28$  in good agreement with the computed 30. The lower curve in the inset of fig. 3 is according to eq. (12) a straight line of slope  $-1$ . The very lowest states deviate, since they “feel” non-constant  $\lambda$  at small  $\rho$ , and the states close to  $E = 0$  deviate due to the influence of the external potential. The energy spectrum becomes even denser above zero energy. For large positive energies in the upper part of the inset the harmonic potential dominates and a straight line with slope  $+1$  is obtained. The small positive energies are influenced by both external trap and interaction potentials.

Using eq. (1) we get  $2\langle\rho^2\rangle = (N-1)\langle r_{12}^2 \rangle \approx 2(N-1)\langle r_i^2 \rangle$ . Even the most bound state,  $\langle\rho^2\rangle^{1/2} \approx 136b$ , has then a root mean square distance between two particles,  $\langle r_{12}^2 \rangle^{1/2} \approx 44b$ , much larger than the interaction range. Also the root mean square radius  $\langle r_i^2 \rangle^{1/2} \approx 31b$  is large.

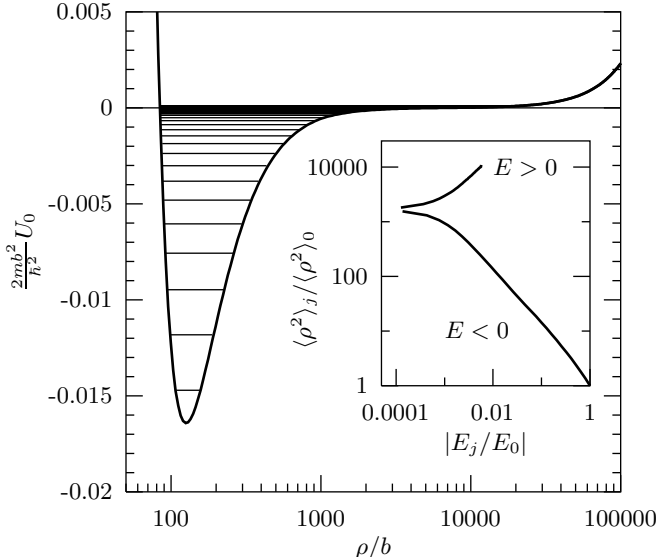


FIG. 3: The lowest radial potential for  $N = 20$ ,  $a_s/b = \infty$ , and  $b_t/b = 1442$ . The horizontal lines indicate the 69 (30 below zero) lowest energy eigenvalues and the inset shows their mean square hyperradii as a function of the absolute value of their energies relative to the values for the lowest state, i.e.  $2mb^2E_0/\hbar^2 \simeq -0.0147$ ,  $\sqrt{\langle\rho^2\rangle_0}/b \simeq 136$ .

At the plateau,  $\lambda \sim \lambda_\infty$ ,  $\xi^2 > 0$  and the radial potential has no intermediate barrier. The centrifugal barrier can only be at  $\rho > \rho_{\text{th}}$ , i.e. in the region where  $\lambda \sim \lambda_{n-c}$ , which provides the estimate of the barrier position  $\rho \sim 2kN^{3/2}|a_s|/3 > \rho_{\text{th}}$ , see eq. (9). A criterion of stability is then obtained by using  $\lambda_{n-c}$  to estimate when the corresponding radial barrier disappears. This yields in analogy to [19] that the condensate will be (meta-) stable if  $N|a_s|/b_t < 0.671$ . This critical value is from the Gross-Pitaevskii equation found to be about 0.6 [2, 23], and recently measured to 0.46 [9] for a  $^{85}\text{Rb}$ -condensate.

Stability is determined by decay through a barrier, like in fig. 2, when negative energy states and the condensate state in the second minimum are present. The tunneling process then populates the states in the first minimum, i.e. many-body states of smaller extension and correspondingly larger density than the initial condensate. Competing with this macroscopic (all particles together) tunneling are the two- and three-particle recombination processes, which can occur from the initial condensate, or more likely from the collapsed many-body states at larger density and smaller  $\rho$ . Thus we have established a decay mechanism, i.e. macroscopic tunneling followed by recombination processes from the intermediate model independent states.

An even more dramatic collapse could be initiated ex-

perimentally by first creating a condensate corresponding to fig. 2, and then suddenly increasing the scattering length to that of fig. 3 [9, 14, 24]. The multi-particle Efimov states of fig. 3 would then quickly be populated, since the barrier is removed, and these states would subsequently leak out of the trap due to recombination.

*Conclusions.* We use a new formulation designed to investigate two-body correlations in boson systems. The qualitative properties of Bose-Einstein condensates are explained by using the hyperspherical adiabatic expansion. Finite range and attractive potentials introduce new features compared to the mean-field approximation. Large scattering lengths are specifically treated. Many-body Efimov states appear for scattering lengths of the order of the trap length as model-independent states of much smaller extension than the condensate. Recombination through these intermediate states is suggested. This opens the possibility for realistic calculations of few-body recombination processes and for macroscopic collapse processes.

---

- [1] O. Sørensen, D. V. Fedorov, A. S. Jensen, and E. Nielsen, cond-mat/0110069.
- [2] F. Dalfovo, S. Giorgini, L. P. Pitaevskii, and S. Stringari, Rev. Mod. Phys. **71**, 463 (1999).
- [3] G. Baym and C. J. Pethick, Phys. Rev. Lett. **76**, 6 (1996).
- [4] V. Efimov, Phys. Lett. B **33**, 563 (1970).
- [5] D. V. Fedorov and A. S. Jensen, Phys. Rev. Lett. **71**, 4103 (1993).
- [6] M. H. Anderson *et al.*, Science **269**, 198 (1995).
- [7] C. C. Bradley, C. A. Sackett, J. J. Tollett, and R. G. Hulet, Phys. Rev. Lett. **75**, 1687 (1995).
- [8] S. L. Cornish *et al.*, Phys. Rev. Lett. **85**, 1795 (2000).
- [9] J. L. Roberts *et al.*, Phys. Rev. Lett. **86**, 4211 (2001).
- [10] E. Nielsen and J. H. Macek, Phys. Rev. Lett. **83**, 1566 (1999).
- [11] B. D. Esry, C. H. Greene, and J. P. Burke, Jr, Phys. Rev. Lett. **83**, 1751 (1999).
- [12] E. Braaten, H.-W. Hammer, and T. Mehen, Phys. Rev. Lett. **88**, 40401 (2002).
- [13] L. P. Pitaevskii, Phys. Lett. A **221**, 14 (1996).
- [14] S. K. Adhikari, cond-mat/0201586.
- [15] D. Blume and C. H. Greene, Phys. Rev. A **63**, 63601 (2001).
- [16] S. Cowell *et al.*, cond-mat/0106628.
- [17] M. F. de la Ripelle, Phys. Lett. **135**, 5 (1984).
- [18] N. Barnea, Phys. Lett. B **446**, 185 (1999).
- [19] J. L. Bohn, B. D. Esry, and C. H. Greene, Phys. Rev. A **58**, 584 (1998).
- [20] N. Barnea, Phys. Rev. A **59**, 1135 (1999).
- [21] A. S. Jensen, E. Garrido, and D. V. Fedorov, Few-Body Systems **22**, 193 (1997).
- [22] E. Nielsen, D. V. Fedorov, A. S. Jensen, and E. Garrido, Phys. Rep. **347**, 373 (2001).
- [23] P. A. Ruprecht, M. J. Holland, K. Burnett, and M. Edwards, Phys. Rev. A **51**, 4704 (1995).
- [24] E. A. Donley *et al.*, Nature **412**, 295 (2001).